Research article

Jigen Chen*, Mengli Liu, Ximei Liu, Yuyi Ouyang, Wenjun Liu* and Zhiyi Wei

The SnSSe SA with high modulation depth for passively Q-switched fiber laser

https://doi.org/10.1515/nanoph-2020-0113
Received February 13, 2020; revised March 3, 2020; accepted March 3, 2020

Abstract: IV–VI semiconductors have attracted widespread attention in basic research and practical applications, because of their electrical and optoelectronic properties comparable to graphene. Herein, an optical modulator based on SnSSe with strong nonlinearity is prepared by chemical vapor transfer method. The modulation depth of proposed SnSSe saturable absorber (SA) is up to 57.5%. By incorporating SnSSe SA into the laser, the Q-switched pulses as short as 547.8 ns are achieved at 1530.07 nm. As far as we know, this is the first successful application of SnSSe in Q-switched lasers. Our investigation not only prove the optical nonlinearity of SnSSe, but also reveal the potential of SnSSe SA in ultrafast photonics.

Keywords: two-dimensional nanomaterials; saturable absorbers; mode-locked laser; fiber lasers.

1 Introduction

In the past few years, Q-switched fiber lasers (QSFL) have made a great progress in practical applications such as optical sensing, material processing, communication, and defense due to their unique advantages in high pulse energy, high cost performance, and compact structure [1–5]. Saturable absorber (SA) is recognized as the key device in passively QSFL, both the structure and categories of which have a crucial impact on the performance of lasers. Since the elimination of dyes, semiconductor saturable absorber mirror (SESAM) as a substitute has dominated the commercial market of SA for more than 20 years [6], the relaxation time, modulation depth, and operating wavelength of which can be accurately engineered. However, the drawbacks such as narrow operating bandwidth, high cost, complex manufacturing processes and low damage thresholds are gradually emerging in the applications and hinder its further development [7–9].

In recent years, some potential saturable materials with excellent properties have emerged as the times require. The excellent properties of ultrafast relaxation time, high damage threshold and broadband absorption capacity of graphene make it shine in the applications [10–13]. In addition to graphene which has set off a research boom, other materials, such as transition metal dichalcogenides (TMDs), black phosphorus (BPs), and topological insulators [14–27], are gradually coming into view. In recent years, TMDs have been the focus of attention, because of the diversity of materials [25–27]. On the one hand, their classical layered structure facilitates the stripping of bulk one into few layers for high-performance optoelectronic devices. On the other hand, the band gap structure of TMDs, which has obvious changes in gap value and indirect-to-direct transition as the thickness decreases, results in some unique properties such as high third-order nonlinear and ultrafast relaxation systems. As the representative of TMDs, molybdenum disulfide (MoS_2) has been widely concerned in optical nonlinearity [28–30]. It has been reported that the MoS_2 nanosheet exhibits a remarkable saturated absorption at 800 nm, which is better than that of graphene [31, 32]. Moreover, the broadband absorption characteristics of MoS_2 have been confirmed from the successful implement of QSFL from 1.06 to 2.1 μm [33].

As a TMD analogue, IV–VI semiconductors have become one of the choices due to their excellent

***Corresponding authors: Prof. Jigen Chen,** Provincial Key Laboratory for Cutting Tools, Taizhou University, Taizhou 318000, China, e-mail: kiddchen@126.com; and **Prof. Wenjun Liu,** State Key Laboratory of Information Photonics and Optical Communications, School of Science, P. O. Box 91, Beijing University of Posts and Telecommunications, Beijing 100876, China; Beijing National Laboratory for Condensed Matter Physics, Institute of Physics, Chinese Academy of Sciences, Beijing 100190, China; and State Key Laboratory of Pulsed Power Laser Technology, National University of Defense Technology, Changsha, Hunan 410073, China, e-mail: jungliu@bupt.edu.cn. https://orcid.org/0000-0001-9380-2990
Mengli Liu, Ximei Liu and Yuyi Ouyang: State Key Laboratory of Information Photonics and Optical Communications, School of Science, P. O. Box 91, Beijing University of Posts and Telecommunications, Beijing 100876, China
Zhiyi Wei: Beijing National Laboratory for Condensed Matter Physics, Institute of Physics, Chinese Academy of Sciences, Beijing 100190, China

characteristics. Because of the influence of the incorporation of sulfur in tin selenium (SnSe) on bandgap tailoring, this ternary compound SnSSe has recently attracted much interest in optoelectronic devices, and has been found to have some advantages in applications. Firstly, the raw materials of SnSSe are abundant and environmentally friendly, which is conducive to large-scale application and commercial production in the future. Secondly, according to the previous research, the interlayer spacing of SnSSe is increased by 2.84% compared with that of SnS_2, which is helpful for the stripping of lamellar materials [34]. In addition, SnSSe grows preferentially along (001) crystal surface, which may be liable for the excellent electrochemical performances. SnSSe has been reported to deliver the highest capacities during the long-term cycling processes compared with other non-composite electrode materials (for example, MoS_2, SnS_2, SWCNT, and etc) [34]. The bandgap energy of 1.08 eV endows the unique advantages in thermoelectric converters and solar cells [35, 36].

In this paper, a stable passively QSFL based on the SnSSe SA is achieved for the first time. The SnSSe SA is manufactured by the chemical vapor transfer (CVT) method and features the large modulation depth up to 57.5%. The repetition rate adjustable from 116.4 to 261.1 kHz, the pulse duration as short as 547.8 ns, the signal-to-noise ratio (SNR) up to 55 dB and pulse energy of 42.79 nJ further confirm the impressive performance of the SnSSe SA in realizing QSFL. Results indicate that the SnSSe SA can be used as a potential nonlinear photonic device.

2 Preparation and characterization

The SnSSe was prepared by the CVT method which has been extensively used in the production of 2D materials with high quality. As previous researches have thoroughly introduced the technological process of CVT [37], we will not go into too much detail here. The prepared SnSSe nanosheets were transferred to the core region of fiber end face with the assistance of polymethyl methacrylate (PMMA) transfer technology. Subsequently, the organic PMMA was removed with acetone as a solvent. So far, the preparation of the SnSSe SA used in this work has been completed.

The surface morphology and thickness of the nanosheets were detected by atomic force microscopy (AFM). The resulting nanosheets are uniform as shown in Figure 1A. From the height difference reflected in Figure 1B, the thickness of SnSSe is about 115 nm. The Raman shift is shown in Figure 1C. The peaks E_g and A_{1g} of SnSSe are located at 137 cm^{-1}, 205 cm^{-1} and 304 cm^{-1}, respectively [38–40]. The peak around 525 cm^{-1} shows silicon from the substrate [41]. The absorption spectrum of SnSSe is shown in Figure 1D. The X-ray photoelectron spectroscopy (XPS) is considered to be an effective method in the determination of elemental composition. The broadband XPS spectrum of SnSSe is shown in Figure 1E. In Figure 1F, the obvious peaks at 54.6 and 53.8 eV are from Se $3d_{3/2}$ and Se $3d_{5/2}$, which demonstrates the divalent selenium exists. Sn 3d spectrum is shown in Figure 1G, two separate peaks located at 495 and 486.6 eV are observed, which are characteristic peaks of Sn $3d_{3/2}$ and Sn $3d_{5/2}$. The distance difference between the two peaks is about 8.4, which demonstrates the existence of Sn. The characteristic peaks of Se $3p_{3/2}$, S 2p and Se $3p_{1/2}$ at 161.6 eV, 163 eV and 166.5 eV are observed in Figure 1H, which indicates that S and Se coexist in the sample. In summary, XPS shows the successful preparation of SnSSe.

By using the balanced twin detector method, the nonlinear absorption characteristics of the SnSSe SA is shown in Figure 1I. The modulation depth of the SnSSe SA is 57.5%, the saturable absorption intensity is 0.065 MW/cm^2, and the non-saturated loss is 25.5%. The insertion loss of the SnSSe SA is 1.3 dB. As shown in Table 1, compared with other saturable absorbing materials, SnSSe has a prominent advantage in large modulation depth.

3 Experiment

Passively QSFL is recognized as an important platform for testing the nonlinearity of SA. The SnSSe-SA is embedded in the erbium-doped fiber (EDF) laser in Figure 2. Wavelength division multiplexer (WDM) incorporates pump light centered at 980 nm into the annular cavity. The length of SMF-28 and EDF is 215 cm and 40 cm, respectively. An optical coupler (OC) with the 20% output ratio is placed after WDM, which is used to monitor the real-time state of output pulses. The polarization state of the light in the cavity and the working state of the system are optimized by fine tuning polarization controller (PC). An isolator (ISO) is added to the fiber laser to guarantee the unidirectional transmission of light.

4 Results and discussion

When the pump power reaches 136.9mW, the Q-switched pulse train is observed on the oscilloscope. Figure 3 shows the various performance of QSFL when the pump power

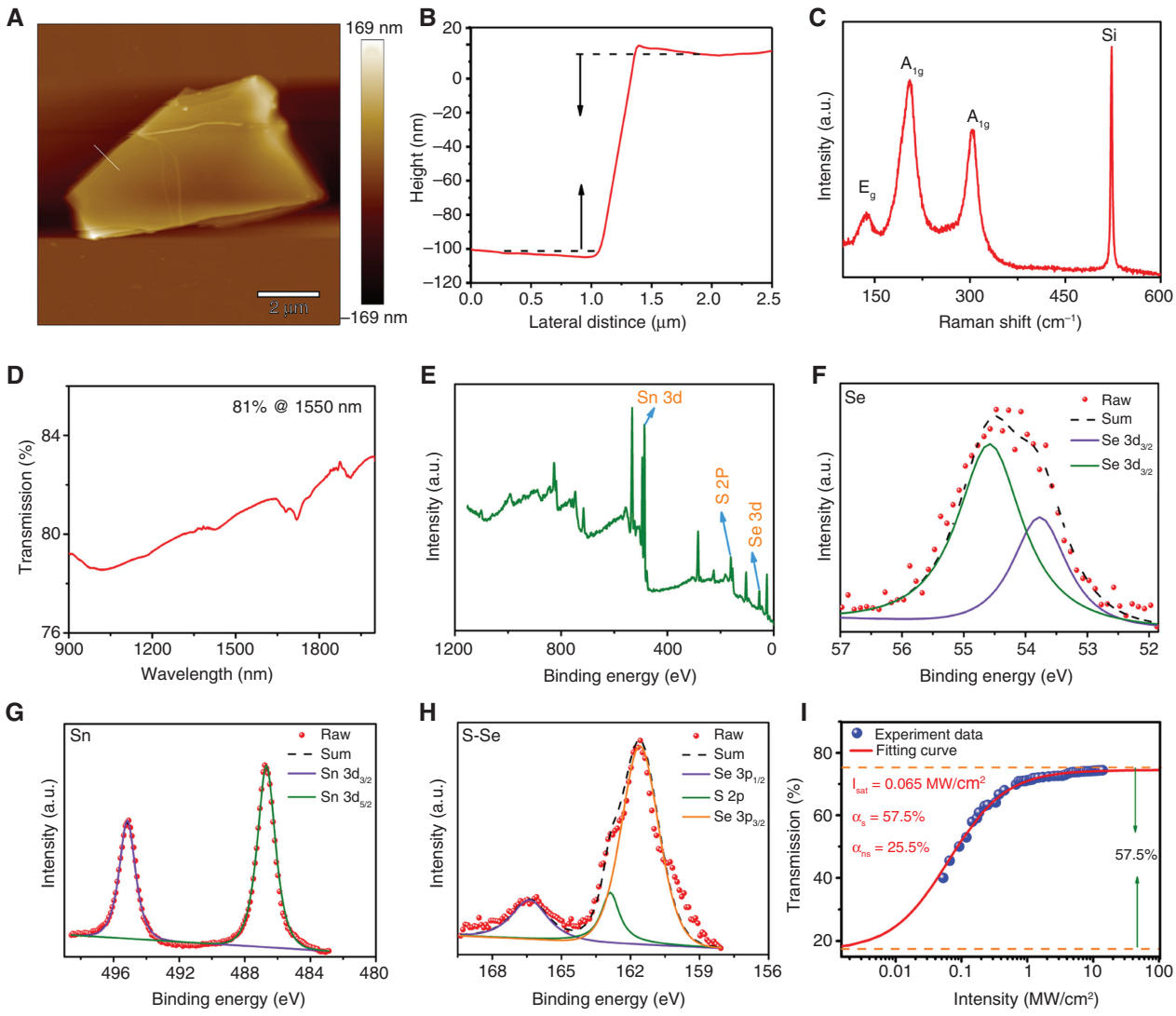

Figure 1: The characterization of SnSSe.
(A) AFM image, (B) Thickness, (C) Raman spectra, (D) Absorption spectrum, (E) Broadband XPS spectrum, (F) XPS spectrum of Se, (G) XPS spectrum of Sn, (H) XPS spectrum of Se-Sn, (I) Nonlinear absorption of SnSSe SA.

Table 1: Nonlinear performance comparison of different SA

Materials	Modulation depth (%)	Saturable absorption intensity (MW/cm²)	Non-saturation loss	Ref.
SCNT	0.94	–	–	[42]
MoS_2	2	10	1%	[43]
$MoSe_2$	6.73	132.5	39.2%	[30]
WS_2	2	27.2	–	[44]
WSe_2	3.5	103.9	75.1%	[22]
BP	8.3	7.9	–	[45]
SnS_2	4.6	125	–	[46]
$SnSe_2$	6.38	–	–	[47]
$CH_3NH_3PbI_3$	5.7	4380	–	[48]
Se	2.13	–	–	[49]
SnS	12.5	83500	37.1%	[50]
SnSSe	57.5	0.065	25.5%	This work

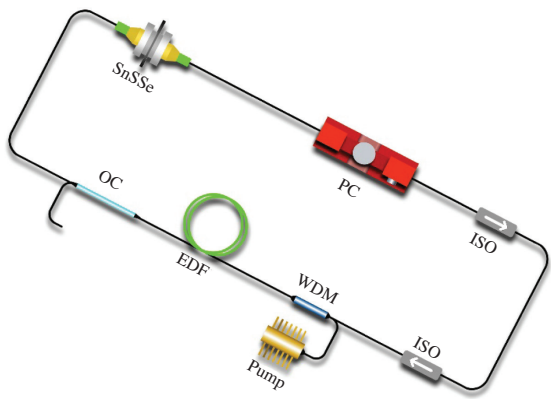

Figure 2: Schematic diagram of QSFL based on SnSSe.

reaches 630 mW. The optical spectrum in Figure 3A indicates that the laser is centered at 1530.07 nm, and the 3 dB spectral width is 2.757 nm. Moreover, the shape of the spectrum remains basically the same in ongoing monitoring, which proves that the working state of the QSFL is stable. Figure 3B demonstrates the different states of QSFL on the oscilloscope at different pump powers. The repetition rate of the Q-switched pulse is reduced from 261.1 kHz to 159.2 kHz with the reduction of pump power from 630 mW to 244.2 mW. The pulse duration as short as 547.8 ns is obtained when the pump power is increased to the maximum of 630 mW in Figure 3C. In Figure 3D, the fundamental frequency of QSFL located at 271.13 kHz, the SNR is as high as 55 dB (RBW is 10 Hz, and the measurement span is 800 kHz), which proves the stability of this QSFL.

In Figure 4A, the repetition rate of the Q-switched pulse increases almost linearly with the increase of pump power from 148 mW to 630 mW. In the primary stage of pump power growth, the pulse duration changes greatly. After that, the change of the pulse duration gradually stabilizes. From Figure 4B, the pulse energy of QSFL changes from 14.51 nJ to 42.79 nJ with the increase of pump power. The maximum output power is 11.14 mW. The damage threshold of the SnSSe SA is about 67.45 mJ/cm^2.

Table 2 demonstrates the performances of QSFLs using different 2D materials as SAs. From Table 2, the pulse duration of enumerated QSFLs are mostly in the μs-level, while that of the pulses obtained in our experiment are ns-level, which indicates that SnSSe-based QSFL has great potential in the achievement of ultrafast laser. As reported in Ref. [54], a high modulation depth is helpful to generate the relatively stable Q-switched pulses. From Table 2, we can see that the laser based on SnSSe with large modulation depth does show the maximum SNR of 55 dB, which indicates the remarkable stability of our Q-switched laser. The reason why the mode locking phenomenon is not

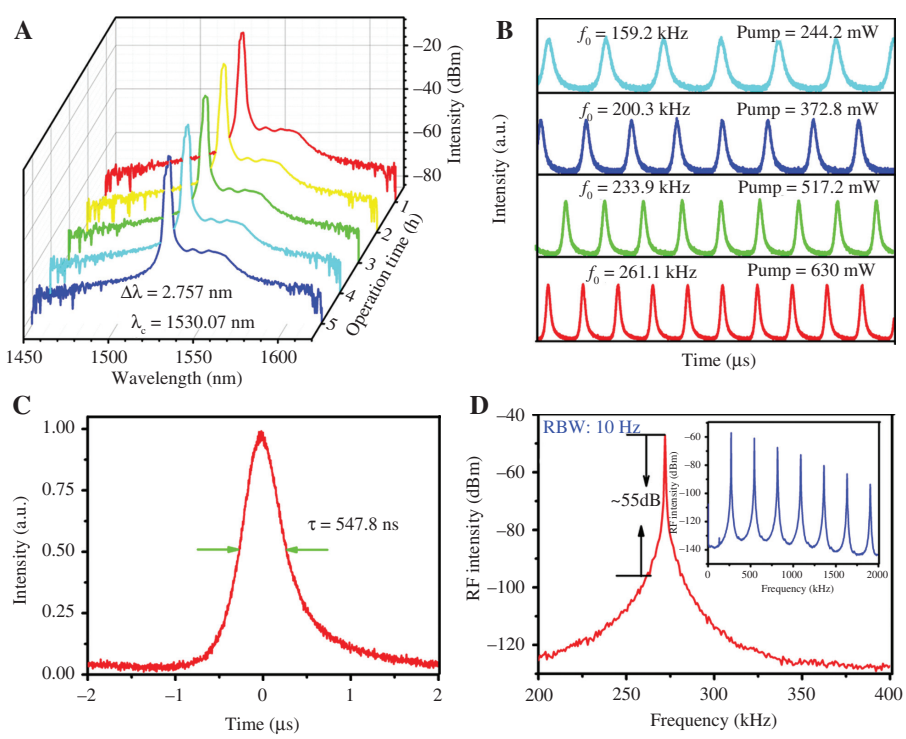

Figure 3: The performance of QSFL.
(A) The optical spectrum. (B) The output pulse sequence at different pump power. (C) The pulse duration of QSFL. (D) RF spectrum.

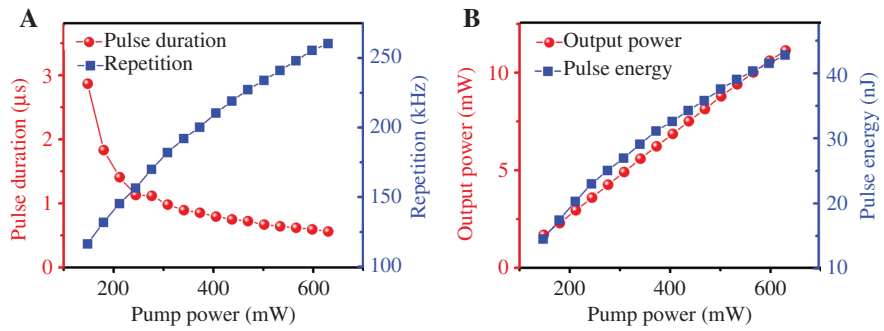

Figure 4: Effect of pump power on laser performance.
The function of the pump power on (A) pulse duration, repetition rate and (B) output power, pulse energy.

Table 2: Performance of QSFLs based on different SA.

Materials	τ (μs)	SNR (dB)	Output power (mW)	Output energy (nJ)	Ref.
BP	13.2	45	–	94.3	[51]
Bi_2Se_3	1.95	48	0.46	17.9	[52]
MoS_2	3.3	–	5.91	160	[43]
$MoSe_2$	4.04	31.3	2.45	–	[30]
WS_2	2.6	43.1	4.1	120	[53]
WSe_2	3.98	46.7	1.23	33.2	[30]
SnSSe	0.5478	55	11.14	42.79	This work

observed here may be that the nonlinearity and dispersion are not balanced in this case.

5 Conclusion

In summary, a QSFL based on the SnSSe SA has been successfully achieved. The SnSSe SA which is prepared by CVT method has owned a large modulation depth of 57.5%. With the change of pump power, the repetition rate of passively QSFL can be adjusted in the range of 116.4 kHz–261.1 kHz. The SNR up to 55 dB has indicated the stability of the system. The maximum output power and pulse energy are 11.14 mW and 42.79 nJ. The minimum pulse duration of 547.8 ns has been proved to be almost at the optimal level. Therefore, as a promising material, SnSSe with strong nonlinearity may be a strong candidate for high performance optoelectronic devices, which also provides a new direction and opportunity for the development of next-generation materials-based devices.

Acknowledgements: This work was supported by the National Natural Science Foundation of China (NSFC) (Grants 11674036, 11875008 and 11975012, Funder Id: http://dx.doi.org/10.13039/501100001809), Beijing Youth Top Notch Talent Support Program (Grant 2017000026833ZK08), Fund of State Key Laboratory of Information Photonics and Optical Communications (Beijing University of Posts and Telecommunications, Grant IPOC2019ZZ01, Funder Id: http://dx.doi.org/10.13039/501100002766), Fundamental Research Funds for the Central Universities (Grant 500419305), State Key Laboratory of Advanced Optical Communication Systems and Networks, Shanghai Jiao Tong University (Grant 2019GZKF03007, Funder Id: http://dx.doi.org/10.13039/501100004921); Beijing University of Posts and Telecommunications Excellent Ph.D. Students Foundation (Grant CX2019202, Funder Id: http://dx.doi.org/10.13039/501100002766); Open Research Fund of State Key Laboratory of Pulsed Power Laser Technology (Grant SKL2018KF04).

References

[1] Popa D, Sun Z, Hasan T, Torrisi F, Wang F, Ferraria AC. Graphene Q-switched, tunable fiber laser. Appl Phys Lett 2011;98:073106.
[2] Niu K, Chen Q, Sun R, Man B, Zhang H. Passively Q-switched erbium-doped fiber laser based on SnS_2 saturable absorber. Opt Mater Express 2017;7:3934–43.
[3] Liu WJ, Liu ML, Han HN, et al. Nonlinear optical properties of WSe_2 and $MoSe_2$ films and their applications in passively Q-switched erbium doped fiber lasers. Photonics Res 2018;6:C15–C21.

[4] Liu ML, Ouyang YY, Hou HR, Liu WJ, Wei ZY. Q-switched fiber laser operating at 1.5 μm based on WTe_2. Chin Opt Lett 2019;17:020006.
[5] Song Y, Shi X, Wu C, Tang D, Zhang H. Recent progress of study on optical solitons in fiber laser. Appl Phys Rev 2019;6:021313.
[6] Weingarten KJ, Kartner FX, Kopf D, et al. Semiconductor saturable absorber mirrors (SESAM's) for femtosecond to nanosecond pulse generation in solid-state lasers. IEEE J Sel Top Quant 1996;2:435–53.
[7] Wang Y, Zhu X, Sheng C, et al. SESAM Q-switched Ho^{3+}-doped ZBLAN fiber laser at 1190 nm. IEEE Photonic Tech L 2017;29: 743–6.
[8] Liu WJ, Liu ML, Lin S, et al. Synthesis of high quality silver nanowires and their applications in ultrafast photonics. Opt Express 2019;27:16440–8.
[9] Liu W, Pang L, Han H, Bi K, Lei M, Wei Z. Tungsten disulphide for ultrashort pulse generation in all-fiber lasers. Nanoscale 2017;9:5806–11.
[10] Sun Z, Martinez A, Wang F. Optical modulators with 2D layered materials. Nat Photonics 2016;10:227–38.
[11] Song Y, Liang Z, Jiang X, et al. Few-layer antimonene decorated microfiber: ultra-short pulse generation and all-optical thresholding with enhanced long term stability. 2D Mater 2017;4:045010.
[12] Zhang Y, Lim CK, Dai Z, et al. Photonics and optoelectronics using nano-structured hybrid perovskite media and their optical cavities. Phys Rep 2019;795:1–51.
[13] Wu L, Xie Z, Lu L, et al. Few-layer tin sulfide: a promising black-phosphorus-analogue 2D material with exceptionally large nonlinear optical response, high stability, and applications in all-optical switching and wavelength conversion. Adv Opt Mater 2018;6:1700985.
[14] Bao Q, Zhang H, Wang Y, et al. Atomic-layer graphene as a saturable absorber for ultrafast pulsed lasers. Adv Funct Mater 2009;19:3077–83.
[15] Zhang H, Tang DY, Zhao LM, Bao QL, Loh KP. Large energy mode locking of an erbium-doped fiber laser with atomic layer graphene. Opt Express 2009;17:17630–5.
[16] Peng KJ, Wu CL, Lin YH, et al. Saturated evanescent-wave absorption of few-layer graphene-covered side-polished single-mode fiber for all-optical switching. Nanophotonics 2018;7:207–15.
[17] Yan PG, Lin R, Ruan S, Liu A, Chen H. A 2.95 GHz, femtosecond passive harmonic mode-locked fiber laser based on evanescent field interaction with topological insulator film. Opt Express 2015;23:154–64.
[18] Zhang H, Liu CX, Qi XL, Dai X, Fang Z, Zhang SC. Topological insulators in Bi_2Se_3, Bi_2Te_3 and Sb_2Te_3 with a single Dirac cone on the surface. Nat Phys 2009;5:438–42.
[19] Sotor J, Sobon G, Macherzynski W, Paletko P, Grodecki K, Abramski KM. Mode-locking in Er-doped fiber laser based on mechanically exfoliated Sb_2Te_3 saturable absorber. Opt Mater Express 2014;4:1–6.
[20] Na D, Park K, Park KH, Song YW. Passivation of black phosphorus saturable absorbers for reliable pulse formation of fiber lasers. Nanotechnol 2017;28:475207.
[21] Han CQ, Yao MY, Bai XX, et al. Electronic structure of black phosphorus studied by angle-resolved photoemission spectroscopy. Phys Rev B 2014;90:085101.
[22] Liu WJ, Pang LH, Han HN, et al. Tungsten disulfide saturable absorbers for 67 fs mode-locked erbium-doped fiber lasers. Opt Express 2017;25:2950–9.
[23] Liu WJ, Liu ML, OuYang YY, Hou HR, Lei M, Wei ZY. CVD-grown $MoSe_2$ with high modulation depth for ultrafast mode-locked erbium-doped fiber laser. Nanotechnol 2018;29:394002.
[24] Liu WJ, Liu ML, Liu B, et al. Nonlinear optical properties of MoS_2-WS_2 heterostructure in fiber lasers. Opt Express 2019;27:6689–99.
[25] Li WY, OuYang Y, Ma G, Liu M, Liu W. Q-switched all-fiber laser with short pulse duration based on tungsten diselenide. Laser Phys 2018;28:055104.
[26] Chen BH, Zhang XY, Guo CS, Wu K, Chen JP, Wang J. Tungsten diselenide Q-switched erbium-doped fiber laser. Opt Eng 2016;55:081306.
[27] Liu ML, Liu WJ, Wei ZY. $MoTe_2$ saturable absorber with high modulation depth for erbium-doped fiber laser. J Lightwave Technol 2019;37:3100–5.
[28] Liu ML, OuYang YY, Hou HR, Lei M, Liu WJ, Wei ZY. MoS_2 saturable absorber prepared by chemical vapor deposition method for nonlinear control in Q-switching fiber laser. Chinese Phys B 2018;27:084211.
[29] Cheng C, Liu H, Tan Y, de Aldana JRV, Chen F. Passively Q-switched waveguide lasers based on two-dimensional transition metal diselenide. Opt Express 2016;24:10385–90.
[30] Chen B, Zhang X, Wu K, Wang H, Wang J, Chen J. Q-switched fiber laser based on transition metal dichalcogenides MoS_2, $MoSe_2$, WS_2, and WSe_2. Opt Express 2015;23:26723–37.
[31] Wang K, Wang J, Fan J, et al. Ultrafast saturable absorption of two-dimensional MoS_2 nanosheets. ACS Nano 2013;7:9260–7.
[32] Du J, Wang Q, Jiang G, et al. Ytterbium-doped fiber laser passively mode locked by few-layer Molybdenum Disulfide (MoS2) saturable absorber functioned with evanescent field interaction. Sci Rep 2014;4:6346.
[33] Luo Z, Huang Y, Zhong M, et al. 1-, 1.5-, and 2-μm fiber lasers Q-switched by a broadband few-layer MoS_2 saturable absorber. J Lightwave Technol 2014;32:4077–84.
[34] Wang X, Chen D, Yang Z, et al. Novel metal chalcogenide SnSSe as a high-capacity anode for sodium-ion batteries. Adv Mater 2016;28:8645–50.
[35] Mahalingam T, Dhanasekaran V, Ravi G, Chandramohand R, Kathalingame A, Rheee J. Role of deposition potential on the optical properties of SnSSe thin films. ECS Transactions 2011;35:1–10.
[36] Perumal P, Ulaganathan RK, Sankar R, et al. Ultra-thin layered ternary single crystals $[Sn(SxSe1-x)_2]$ with bandgap engineering for high performance phototransistors on versatile substrate. Adv Funct Mater 2016;26:3630–8.
[37] Liu W, Liu M, Wang X, et al. Thickness-dependent ultrafast photonics of SnS_2 nanolayers for optimizing fiber lasers. ACS Appl Nano Mater 2019;2:2697–705.
[38] Wang X, Li C, Liu C, et al. Highly faceted layered orientation in SnSSe nanosheets enables facile Li^+-diffusion channels. Electrochim Acta 2019;318:937–48.
[39] Huang W, Xie Z, Fan T, et al. Black-phosphorus-analogue tin monosulfide: an emerging optoelectronic two-dimensional material for high-performance photodetection with improved stability under ambient/harsh conditions. J Mater Chem C 2018;6:9582–93.

[40] Xie Z, Wang D, Fan T, et al. Black phosphorus analogue tin sulfide nanosheets: synthesis and application as near-infrared photothermal agents and drug delivery platforms for cancer therapy. J Mater Chem B 2018;6:4747–55.
[41] Zhou X, Li J, Leng Y, Cong X, Liu D, Luo J. Exploring interlayer interaction of $SnSe_2$ by low-frequency Raman spectroscopy. Physica E 2019;105:7–12.
[42] Kivistö S, Hakulinen T, Kaskela A, et al. Carbon nanotube films for ultrafast broadband technology. Opt Express 2009;17:2358–63.
[43] Huang YZ, Luo ZQ, Li YY, et al. Widely-tunable, passively Q-switched erbium-doped fiber laser with few-layer MoS_2 saturable absorber. Opt Express 2014;22:25258–66.
[44] Li L, Wang YG, Wang ZF, Wang X, Yang GW. High energy Er-doped Q-switched fiber laser with WS_2 saturable absorber. Opt Commun 2018;406:80–4.
[45] Zhao R, He J, Su X, et al. Tunable high-power Q-switched fiber laser based on BP-PVA saturable absorber. IEEE J Sel Top Quant Electron 2017;24:0900405.
[46] Niu K, Sun R, Chen Q, Man B, Zhang H. Passively mode-locked Er-doped fiber laser based on SnS_2 nanosheets as a saturable absorber. Photonics Res 2018;6:72–6.
[47] Liu JS, Li XH, Guo YX, et al. $SnSe_2$ nanosheets for subpicosecond harmonic mode-locked pulse generation. Small 2019;15:1902811.
[48] Li P, Chen Y, Yang T, et al. Two-dimensional $CH_3NH_3PbI_3$ perovskite nanosheets for ultrafast pulsed fiber lasers. ACS Appl Mater Inter 2017;9:12759–65.
[49] Xing C, Xie Z, Liang Z, et al. 2D nonlayered selenium nanosheets: facile synthesis, photoluminescence, and ultrafast photonics. Adv Opt Mater 2017;5:1700884.
[50] Xie Z, Zhang F, Liang Z, et al. Revealing of the ultrafast third-order nonlinear optical response and enabled photonic application in two-dimensional tin sulfide. Photonics Res 2019;7:494–502.
[51] Chen Y, Jiang GB, Chen SQ, et al. Mechanically exfoliated black phosphorus as a new saturable absorber for both Q-switching and mode-locking laser operation. Opt Express 2015;23:12823–33.
[52] Luo ZQ, Huang YZ, Weng J, et al. 1.06 μm Q-switched ytterbium-doped fiber laser using few-layer topological insulator Bi_2Se_3 as a saturable absorber. Opt Express 2013;21:29516–22.
[53] Lau KY, Latif AA, Bakar MHA, Muhammad FD, Omar MF, Mahdi MA. Mechanically deposited tungsten disulfide saturable absorber for low-threshold Q-switched erbium-doped fiber laser. Appl Phys B 2017;123:221.
[54] Hönninger C, Paschotta R, Morier-Genoud F, Moser M, Keller U. Q-switching stability limits of continuous-wave passive mode locking. J Opt Soc Am B 1999;16:46–56.